Neuron, Vol. 36, 881–889, December 5, 2002, Copyright ©2002 by Cell Press

Subunit Stoichiometry of the CNG Channel of Rod Photoreceptors

Dietmar Weitz,[1,4] Nicole Ficek,[1,4] Elisabeth Kremmer,[2] Paul J. Bauer,[1] and U. Benjamin Kaupp[1,3]
[1]Institut für Biologische Informationsverarbeitung
Forschungszentrum Jülich
52425 Jülich
Germany
[2]Institut für Molekulare Immunologie
GSF
Marchioninistr. 25
81377 München
Germany

Summary

Cyclic nucleotide-gated (CNG) channels play a central role in the conversion of sensory stimuli into electrical signals. CNG channels form heterooligomeric complexes built of A and B subunits. Here, we study the subunit stoichiometry of the native rod CNG channel by chemical crosslinking. The apparent molecular weight (M_w) of each crosslink product was determined by SDS-PAGE, and its composition was analyzed by Western blotting using antibodies specific for the A1 or B1 subunit. The number of crosslink products and their M_w as well as the immunological identification of A1 and B1 subunits in the crosslink products led us to conclude that the native rod CNG channel is a tetramer composed of three A1 and one B1 subunit. This is an example of violation of symmetry in tetrameric channels.

Introduction

Cyclic nucleotide-gated (CNG) channels control the flow of cations across the plasma membrane of photoreceptor cells and olfactory neurons (Burns and Baylor, 2001; Kaupp and Seifert, 2002). In photoreceptor cells, a light-driven decrease in cGMP concentration leads to a closure of CNG channels and results in a hyperpolarization of the membrane potential. In olfactory neurons, binding of odorants to their receptor induces an increase in cAMP concentration, which leads to the opening of a CNG channel, and thereby produces a depolarization of the membrane potential. CNG channels are also expressed in several other tissues where their function remains to be established (for reviews see Richards and Gordon, 2000; Kaupp and Seifert, 2002).

CNG channels form heteromeric complexes comprising several distinct subunits. Biochemical studies and molecular cloning revealed two different types of subunits, commonly referred to as A and B subunits. Both types of subunits share a similar topology with voltage-gated potassium channels characterized by six transmembrane segments S1–S6 (Kaupp et al., 1989; Wohlfart et al., 1992; Henn et al., 1995) and a pore-forming loop between S5 and S6 (Goulding et al., 1993; Seifert et al., 1999; for reviews, see Flynn and Zagotta, 2001; Kaupp and Seifert, 2002). This structural similarity suggested that CNG channels, like K^+ channels (MacKinnon, 1991), exist as tetramers of unknown stoichiometry. The strategy taken to examine the number of subunits has been to express wild-type and mutant subunits. The mutants are expected to change the electrophysiological properties in characteristic ways and thereby report the number and arrangement of subunits in the channel complex. This approach provided evidence for a tetrameric arrangement of subunits (Gordon and Zagotta, 1995; Liu et al., 1996; Varnum and Zagotta, 1996). A low-resolution structure of the native rod channel obtained by single-particle electron microscopy also suggests a tetrameric structure (Higgins et al., 2002). However, the spatial resolution was not sufficient to visualize individual subunits in the channel complex.

CNG channels of rod and cone photoreceptor cells are built from two distinct subunits (A1/B1a and A3/B3, respectively) (Chen et al., 1993; Bönigk et al., 1993; Körschen et al., 1995; Gerstner et al., 2000), whereas CNG channels of olfactory neurons are built from three different subunits (A2/A4/B1b) (Sautter et al., 1998; Bönigk et al., 1999; Bradley et al., 2001). The arrangement of recombinant A1 and B1 subunits has been studied previously by heterologous expression. It was concluded that channels comprise two A1 and two B1 subunits and that like subunits are adjacent to each other (A1-A1-B1-B1) (Shammat and Gordon, 1999). This result was questioned by He and collaborators, who proposed a diagonal arrangement of subunits (A1-B1-A1-B1) (He et al., 2000). However, the stoichiometric composition and arrangement of subunits in the native heteromeric channels needs to be established.

In this study, we examined the stoichiometry of the native rod CNG channel by chemical crosslinking of subunits, followed by analysis of crosslink products with specific antibodies against the A1 and B1 subunits. In contrast to previous studies, we find that the native CNG channel of rods is a tetrameric complex comprising three A1 and one B1 subunit.

Results

Stoichiometry of the Rod CNG Channel

The native rod CNG channel consists of A1 and B1 subunits. For a tetrameric arrangement, three different subunit compositions are conceivable: three A1 and one B1 subunit (Figure 1C, model I), two A1 and two B1 subunits (model II), or one A1 and three B1 subunits (not shown). The model with one A1 and three B1 subunits can be excluded, because a dimer of A1 subunits has been shown in a previous study using crosslinking (Schwarzer et al., 2000). We used chemical crosslinking to determine the number of each subunit type in the channel complex. Models I and II predict characteristic differences in the pattern and composition of crosslink products. First, the total number of crosslink products

[3]Correspondence: a.eckert@fz-juelich.de
[4]These authors contributed equally to this work.

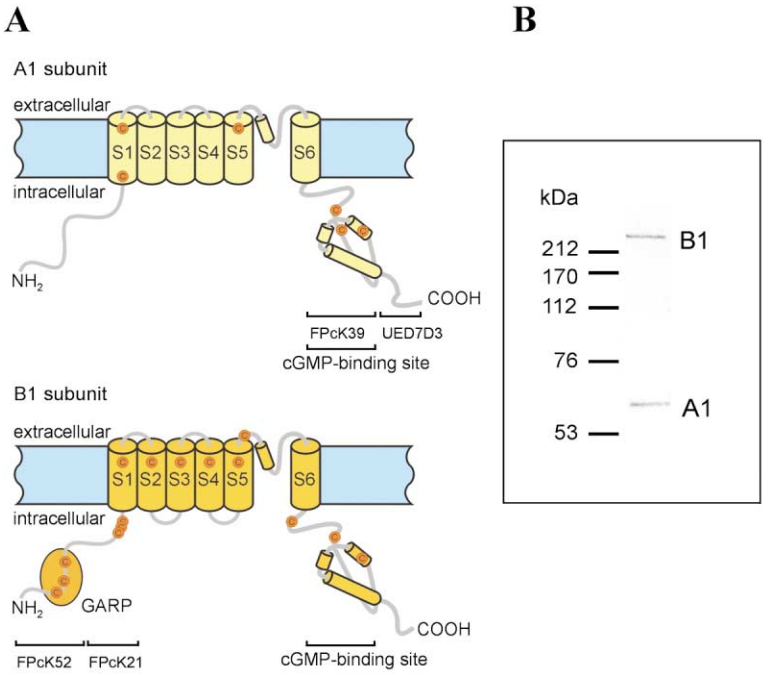

Figure 1. Membrane Topology of the A1 and B1 Subunits

(A) The A1 and B1 subunits share a transmembrane topology involving six membrane-spanning segments (S1–S6), a pore region between S5 and S6, and a cyclic nucleotide binding domain at the C terminus. The B1 subunit has a glutamic acid-rich protein (GARP) domain at the N terminus. The A1 and B1 subunits carry 6 and 15 cysteine residues, respectively. The different epitopes of the antibodies FPcK21, FPcK39, FPcK52, and UED7D3 are indicated.

(B) Purified CNG channel (1.2 μg) studied by SDS-PAGE and Coomassie staining. The apparent M_w of the A1 and the B1 subunit are 63 kDa and 240 kDa, respectively.

(C) Crosslink products predicted by two different models of subunit composition: 3A1-1B1 stoichiometry (left), 2A1-2B1 stoichiometry (right).

C

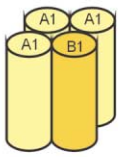

	kDa	anti-A1	anti-B1
3A1-1B1	429	+	+
2A1-1B1	366	+	+
1A1-1B1	303	+	+
B1	240	-	+
3A1	189	+	-
2A1	126	+	-
A1	63	+	-

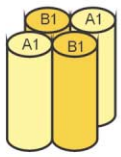

	kDa	anti-A1	anti-B1
2A1-2B1	606	+	+
1A1-2B1	543	+	+
2B1	480	-	+
2A1-1B1	366	+	+
1A1-B1	303	+	+
B1	240	-	+
2A1	126	+	-
A1	63	+	-

differs between the two models (five for model I and six for model II). Second, model I predicts for the fully crosslinked end product an apparent molecular weight (M_w) of 429 kDa, while model II predicts a M_w of 606 kDa. Third, some intermediate crosslink products are shared by the two models, while others are unique for either one of the models. For example, a trimer of the A1 subunit and the 3A1-1B1 crosslink are predicted by model I, whereas a dimer of the B1 subunit as well as crosslinks (of A1) with this dimer (1A1-2B1, 2A1-2B1) are predicted by model II. Each crosslink product can be identified by both its M_w and its subunit composition (only A1, only B1, or both A1 and B1). We studied the subunit stoichiometry of the native channel protein in the membrane as well as that of the purified channel protein in detergent solution. We used two different crosslink reagents—amino-specific and thiol-specific—and at least two different antibodies for each subunit type.

Thiol-Specific Crosslinking of the CNG Channel in the Membrane of Rods

We crosslinked the channel in the native plasma membrane using the thiol-specific reagent 1,4-Bismaleimidyl-2,3-dihydroxybutane (BMDB). BMDB is a homobifunctional dimaleimide reagent that crosslinks adjacent cysteines. The A1 and B1 subunits carry 6 and 15 cysteine residues, respectively (Figure 1A). In the B1 subunit, the cysteine residues are regularly distributed over the entire polypeptide chain, while in the A1 subunit, 3 of 6 cysteine residues are located in the transmembrane region. Three cysteine residues are located in or nearby the cyclic nucleotide binding domain.

The rod CNG channel is either associated with or in close proximity to other proteins, e.g., calmodulin, the Na^+/Ca^{2+}-K^+ exchanger, peripherin, and the rim protein (Hsu and Molday, 1993; Molokanova et al., 1997; Körschen et al., 1999; Schwarzer et al., 2000; Poetsch

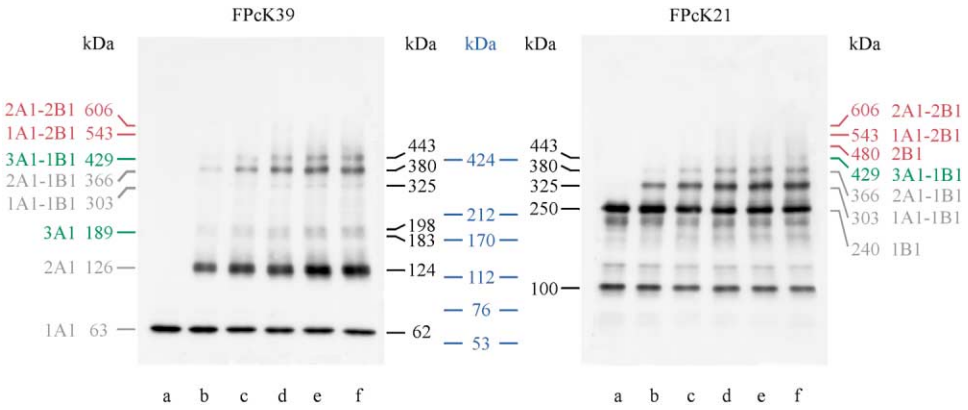

Figure 2. Thiol-Specific Crosslinking of the CNG Channel in ROS Membranes

Hypotonically washed and NEM-treated ROS membranes were incubated with 50 μM BMDB in the presence of 50 μM 8-Br-cGMP (lanes a–f). The crosslink reaction was stopped after different incubation times (0, 1, 3, 5, 7, and 20 hr). Crosslink products (75 μg protein in each lane) were separated by 3.5%–7.5% SDS-PAGE and transferred to Immobilon membranes. Left, the Western blot was labeled with the polyclonal antibody FPcK39, directed against the A1 subunit. Right, the same blot labeled with the polyclonal antibody FPcK21, directed against the B1 subunit. The position of the marker proteins is depicted in blue between the two blots. The measured M_w of each band is shown at the right and left side, respectively, of the blots. The M_w of crosslink products predicted by models I and II are marked on the left and right sides, respectively, of each blot: green bands specific for model I, red bands specific for model II, and gray bands common for both models. The position of the predicted crosslink products on the Western blot were deduced by linear interpolation from a plot of the log M_w of the standard proteins against their relative mobility on the SDS polyacrylamide gel.

et al., 2001). In order to prevent crosslinks of the CNG channel with interacting proteins and to reduce unspecific "background," we used the following experimental protocol (Schwarzer et al., 2000). ROS membranes were first washed several times in hypotonic Ca^{2+}-free buffer to remove soluble proteins. The membranes were then incubated with the thiol-modifying reagent N-ethylmaleimide (NEM) to block accessible thiol groups of the CNG channel and of other proteins. NEM incubation was terminated with dithiothreitol (DTT); excess DTT was subsequently removed by washing membranes with isotonic buffer. 8-Br-cGMP was added to the CNG channel to expose previously inaccessible cysteine residues in the A1 subunit (Serre et al., 1995; Gordon et al., 1997; Brown et al., 1998; Schwarzer et al., 2000; Zheng and Zagotta, 2000; Rosenbaum and Gordon, 2002). This procedure ensures that cysteine residues that are inaccessible in the absence of 8-Br-cGMP become available for the crosslink reaction.

Crosslinking with BMDB was allowed to proceed for 1, 3, 5, 7, and 20 hr. Crosslink products were separated by SDS-PAGE and the M_w and the composition of each crosslink product was analyzed using anti-A1 (Figure 2, left) and anti-B1 antibodies on one and the same Western blot (Figure 2, right). Incubation of the channel protein with the crosslink reagent for increasing periods of time resulted in the gradual formation of various intermediate products up to an end product. Lane a shows noncrosslinked membranes (control), and lanes b–f show the appearance of crosslink products with incubation time.

Even after 20 hr incubation time, approximately 50% of the A1 and B1 monomers are still present, suggesting that crosslinking of cysteines made accessible by 8-Br-cGMP is slow. The anti-A1 antibody (FPcK39) recognized bands with a M_w of 62 kDa, 124 kDa, 325 kDa, 380 kDa, and 443 kDa, and a double band at 183/198 kDa (Figure 2, left). The double band at 183/198 kDa and the band at 325 kDa were only weakly labeled but became clearly visible after a longer exposure time of the film. The anti-B1 antibody (FPcK21) recognized the B1 monomer with a M_w of 250 kDa and crosslink bands at 325 kDa, 380 kDa, and 443 kDa (Figure 2, right). The minor bands below 250 kDa represent proteolytically cleaved degradation products or a splice variant of the B1 subunit (~100 kDa), which have also been observed before (Schwarzer et al., 2000). These fragments are not recognized by another anti-B1 antibody (FPcK52) directed against the GARP region of the B1 subunit (Figure 3, right, see below) and do not contribute to any of the major crosslink products.

The crosslink products are consistent with predictions from model I (three A1 subunits, one B1 subunit). First, the bands of 62 kDa, 124 kDa, and 183/198 kDa, which are only detected by the anti-A1 antibody, display the predicted M_w of the monomer, dimer, and trimer of the A1 subunit, respectively. The observation of higher-order crosslinks indicates that more than one cysteine becomes accessible upon channel activation. The double band is probably due to the formation of different intermolecular or even intramolecular crosslinks. A similar behavior has been described in other crosslink studies (Schulteis et al., 1996; Raab-Graham and Vandenberg, 1998). The distances between these three bands (60–70 kDa) equal the approximate size of one A1 subunit (63 kDa). Crosslink products with a M_w larger than the B1 subunit (240 kDa) were recognized by antibodies against both subunits, i.e., these products consist of A1 and B1 subunits. The difference in M_w between bands again amounts to the size of one A1 subunit.

The crosslink pattern is inconsistent with model II in several respects. First, the anti-B1 antibody recognized four bands, whereas model II predicts six bands. Second, no crosslink products ≥440 kDa were recognized

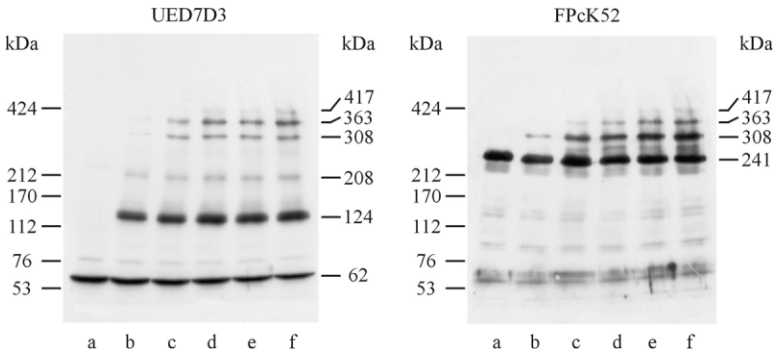

Figure 3. Thiol-Specific Crosslinking of the CNG Channel in ROS Membrane: Detection by Different Antibodies

Left, Western blot labeled with the monoclonal anti-A1 antibody UED7D3. Right, same Western blot labeled with the polyclonal anti-B1 antibody FPcK52. All other conditions are as in Figure 2.

by either the anti-A1 antibody or the anti-B1 antibody, whereas model II predicts in this range two bands with anti-A1 (563 and 626 kDa) and three bands with anti-B1 (480, 563, and 626 kDa). These results argue that the native CNG channel of rod photoreceptors consists of three A1 and one B1 subunit.

The failure of antibodies FPcK39 and FPcK21 to detect crosslink products predicted by model II might be due to masking of epitopes by the crosslink reaction. To test for this possibility and to provide further evidence for a 3A1-1B1 stoichiometry, we employed another set of antibodies that were raised against other epitopes of the respective subunit. Monoclonal antibody UED7D3 recognizes the C-terminal region of the A1 subunit, whereas FPcK39 recognizes the cNMP binding domain. Antibody FPcK52 recognizes the N-terminal GARP region of B1, whereas FPcK21 recognizes the N-terminal region of the β' part of B1 (see also Körschen et al., 1995). Antibodies UED7D3 and FPcK52 recognized a pattern of crosslink products similar to that recognized by antibodies FPcK39 and FPcK21 (Figure 3). In particular, FPcK52 and FPcK21 produced the same band pattern for $M_w \geq 240$ kDa, yet FPcK52 did not detect degradation products of B1 < 240 kDa. This result demonstrates that the small amount of B1 fragments does not affect the formation of the major crosslink products.

We have also probed the blot with antibodies against the Na^+/Ca^{2+}-K^+ exchanger and peripherin, two membrane proteins that are known to interact with the CNG channel in the plasma membrane (Molday and Molday, 1998; Schwarzer et al., 2000; Poetsch et al., 2001). We could not detect crosslinks between CNG channel subunits and these two proteins using NEM-treated membranes (data not shown). Thiol-specific crosslinking of the CNG channel in the ROS membrane without previous blocking of accessible thiol groups revealed bands corresponding to the monomer, dimer, and trimer of the A1 subunit and the B1 monomer at 250 kDa. However, at higher molecular weights, the anti-A1 and the anti-B1 antibodies detected a diffuse "smear," which obscured the detection of discrete bands (data not shown). The smear is probably caused by numerous crosslinks with other proteins in the ROS membrane including the Na^+/Ca^{2+}-K^+ exchanger and peripherin (Schwarzer et al., 2000; Poetsch et al., 2001).

Amino-Specific Crosslinking of the CNG Channel in the Membrane of Rods

Another matter of concern was that some crosslink products might be underrepresented due to steric hindrance or lack of cysteines. To test for this possibility, we used Bis(sulfosuccinimidyl)suberate (BS^3), a homobifunctional crosslinker with two N-hydroxysuccinimidester as reactive groups. Succinimidester react with free amino groups in proteins, preferentially with the ϵ-amino group of lysine residues. The crosslink reaction was stopped after 1, 2, 5, 10, and 30 min. Figure 4 shows a Western blot of ROS membranes after crosslinking with BS^3. The blot was labeled with antibodies against the A1 (left) and B1 subunit (middle). Both antibodies detected a similar pattern of crosslink products as was observed for thiol-specific crosslinking, including the appearance of double bands. However, one difference was noticeable. Both antibodies recognized an additional crosslink product of approximately 640 kDa. Reprobing the Western blot with an antibody against the Na^+/Ca^{2+}-K^+ exchanger confirmed that the 640 kDa band was due to a crosslink between channel subunits and the Na^+/Ca^{2+}-K^+ exchanger (right). Association of the CNG channel and the Na^+/Ca^{2+}-K^+ exchanger has been reported previously (Molday and Molday, 1998; Schwarzer et al., 2000; Poetsch et al., 2001).

In conclusion, amino-specific crosslinking provides further evidence for a 3A1-1B1 stoichiometry. The crosslinker BS^3 favors crosslinks among the CNG channel subunits and creates only minor crosslink products with other membrane proteins.

Thiol- and Amino-Specific Crosslinking of Purified CNG Channel

To rigorously test whether the association of the CNG channel with neighboring proteins in the ROS membrane—may it be specific or unspecific—is compromising our conclusions, we studied the thiol- and amino-specific crosslinking in the solubilized and purified channel protein (Figure 1B). Crosslinking with BMDB (Figure 5) and BS^3 (Figure 6) resulted in similar patterns of crosslink products. We performed a time series of the crosslink reaction with BMDB on the purified channel protein in the presence of 8-Br-cGMP. The anti-A1 antibody detected the A1 monomer (64 kDa) and crosslink products of 126 kDa, 178 kDa, 309 kDa, 363 kDa, and 440 kDa (Figure 5, left). The bands at 178 kDa and 309 kDa were only weakly labeled and yet, after longer exposition, they became clearly visible. The anti-B1 antibody recognized the B1 monomer at 250 kDa and bands with M_w of 309 kDa, 363 kDa, and 440 kDa (Figure 5, right) that were also recognized by the anti-A1 antibody. Additionally, the anti-B1 antibody recognized a faint band at 280

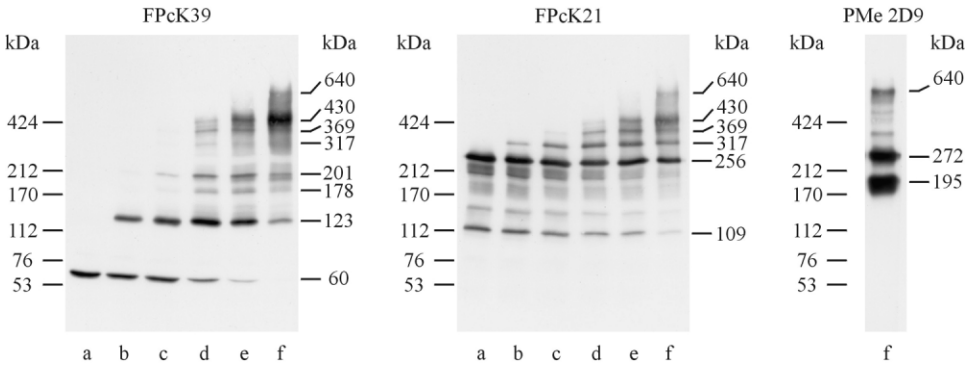

Figure 4. Amino-Specific Crosslinking of CNG Channel in ROS Membranes

Hypotonically washed membranes were incubated with 0.5 mM BS^3 (lanes a–f). The crosslink reaction was stopped after different incubation times (0, 1, 2, 5, 10, and 30 min). Crosslink products (75 μg protein in each lane) were separated by 3.5%–7.5% SDS-PAGE and transferred to Immobilon membranes. Left, the Western blot was labeled with the monoclonal anti-A1 antibody FPcK39. Middle, the same blot labeled with the polyclonal anti-B1 antibody FPcK21. Right, lane f of the same plot labeled with the monoclonal antibody PMe 209 against the Na^+/Ca^{2+}-K^+ exchanger.

kDa. Because this band is not recognized by the anti-A1 antibody and because no additional proteins with a M_w of approximately 30–40 kDa are present in the purified channel sample, we presume that this additional band is due to an intramolecular crosslink in the B1 subunit that lowers its electrophoretic mobility.

In addition, we performed a time series of the crosslink reaction with BS^3 on the purified channel protein. The anti-A1 antibody recognized bands with M_w of 66 kDa, 190 kDa, 310 kDa, 365 kDa, and 430 kDa and a double band at 125/133 kDa (Figure 6, left). The bands with M_w of 190 kDa and 310 kDa were only weakly labeled, but became clearly visible after longer exposition of the film. The anti-B1 antibody recognized the B1 monomer with a M_w of 250 kDa and the crosslink bands at 310 kDa, 365 kDa, and 430 kDa (Figure 6, right), which were also recognized by the anti-A1 antibody. Even after long exposition times, no products of $M_w \geq 430$ kDa have been observed. In summary, thiol-specific and amino-specific crosslinking of the purified CNG channel results in crosslink products predicted by model I, i.e., three A1 and one B1 subunit.

Discussion

In this study, we investigated the subunit stoichiometry of the native CNG channel of rods by chemical crosslinking. While our analysis was focused on the differences predicted by two different models (3A1-1B1 versus 2A1-2B1), the crosslinking approach is independent of the specific models chosen. Table 1 summarizes the results of 23 crosslinking experiments with native ROS membranes as well as purified channel protein, using two different crosslinking reagents (BS^3 and BMDB). Altogether, these results show that the native rod CNG channel is a tetrameric complex composed of three A1 and

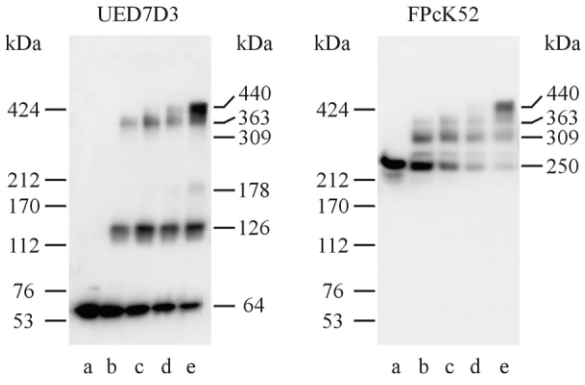

Figure 5. Thiol-Specific Crosslinking of the Solubilized and Purified CNG Channel

Purified CNG channel (300 ng) was crosslinked with 5 μM BMDB in the presence of 200 μM 8-Br-cGMP (lanes a–e). The crosslink reaction was stopped after different incubation times (0, 10, 20, 30, and 60 min). Crosslink products were separated by 3%–7.5% SDS-PAGE and transferred to Immobilon membranes. Left, the Western blot was labeled with the monoclonal anti-A1 antibody UED7D3. Right, the same blot labeled with the polyclonal anti-B1 antibody FPcK52.

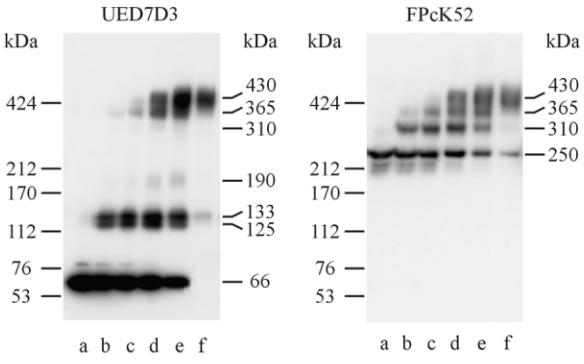

Figure 6. Amino-Specific Crosslinking of the Solubilized and Purified CNG Channel

Purified CNG channel (300 ng) was crosslinked with 0.5 mM BS^3 (lanes a–f). The crosslink reaction was stopped after different incubation times (0, 1, 2, 5, 10, and 30 min). Crosslink products were separated by 3%–7.5% SDS-PAGE and transferred to Immobilon membranes. Left, the Western blot was labeled with the monoclonal anti-A1 antibody UED7D3. Right, the same blot labeled with the polyclonal anti-B1 antibody FPcK52.

Table 1. Summary of the Results of Crosslink Experiments

Crosslink Products	M_w (kDa)[a]	ΔM_w (kDa)[b]	Predicted M_w[c]	Anti-A1	Anti-B1
3A1-1B1	429 ± 11	61	429	+	+
2A1-1B1	368 ± 10	56	366	+	+
A1-B1	312 ± 10	67	303	+	+
B1	245 ± 11	–	240	–	+
3A1	193 ± 10	71	189	+	–
2A1	122 ± 10	61	126	+	–
A1	61 ± 4	–	63	+	–

[a] Mean ± SD were calculated from 23 experiments using either BS^3 or BMDB as crosslinking reagent.
[b] ΔM_w, difference in M_w between two crosslink products.
[c] Model I, three A1 and one B1 subunit.

one B1 subunit. It is unlikely that subunits other than A1 and B1 participate in channel formation, because experiments with the native membrane and the purified channel protein result in similar crosslink products.

Several caveats intrinsic to chemical crosslinking and identification of crosslink products by Western blot analysis could lead to misinterpretations of the results. One problem concerns the lower blotting efficiency of large compared to small proteins. Consequently, crosslink products of higher M_w might be either underrepresented or missed altogether. However, under our experimental conditions, marker proteins with M_w of 424 kDa (myosin dimer), 636 kDa (myosin trimer), and 760 kDa (nebulin) were readily blotted onto the PVDF membrane. Moreover, no additional crosslink products with $M_w \geq 424$ kDa were detected when using 3%–5% gradient gels, which should facilitate blotting of proteins. Another caveat concerns epitope masking by the covalent modification of amino acids. We alleviated this potential difficulty by using different crosslink reagents (amino- and thiol-specific), which are likely to react with different regions in the protein, and by using different polyclonal and monoclonal antibodies raised against different domains. Notwithstanding, we have noticed partial epitope masking with respect to the 312 kDa band corresponding to the A1-B1 crosslink product. This band was weakly labeled with both anti-A1 antibodies, while the anti-B1 antibodies strongly labeled this band.

Our results disagree with previous studies that proposed a 2A1-2B1 stoichiometry (Shammat and Gordon, 1999; He et al., 2000). The stoichiometry and arrangement of subunits was inferred from electrophysiological properties of recombinant channels. In one study, the potentiation of CNG channel activity by Ni^{2+} was used as a molecular ruler to probe the topology of subunits (Shammat and Gordon, 1999). These authors proposed an A1-A1-B1-B1 arrangement of subunits. The approach rests on the finding that Ni^{2+} potentiation involves two sites (histidine residues) in the C-linker region of *adjacent* A1 subunits (Gordon and Zagotta, 1995). This requirement was established for homomeric A1 tandem constructs but has not been independently tested in heteromeric channels. In fact, He and coworkers (He et al., 2000) demonstrated that Ni^{2+} potentiation is mediated by the B1 subunit in the absence of key histidines in the A1 subunit. Furthermore, Ni^{2+} potentiation persisted when putative Ni^{2+} binding sites in the C-linker region of the B1 subunit have been eliminated. He and coworkers proposed a diagonal A1-B1-A1-B1 arrangement of channel subunits by comparing the electrophysiological properties of different tandem constructs used to constrain the arrangement of subunits in the channel complex (He et al., 2000).

For the following reasons, the interpretation of electrophysiological properties in terms of the stoichiometry and topology of subunits in a channel complex is equivocal. The approach using tandem constructs tacitly assumes that the channel contains an *even* number of subunits (i.e., excludes pentamers) and an *equal* number of A and B subunits. It is unlikely to provide structural information for a channel complex composed of three A and one B subunit. Moreover, McCormack and coworkers (McCormack et al., 1992) show that tandem constructs do not ensure the formation of channels with the expected stoichiometry. In their studies on wt and mutant *Shaker* K^+ channels, only the leading subunit of a tandem construct was incorporated into the channel complex, irrespective of whether it was wt or mutant. In another study, Sukharev and coworkers disclosed a pentameric structure of the native mechano-sensitive MscL channel from *Escherichia coli* by various biochemical techniques (Sukharev et al., 1999), in good agreement with the crystal structure of the MscL channel from *Mycobacterium tuberculosis* (Chang et al., 1998). However, the heterologous expression of both tandem and triple constructs gave rise to channels with native properties, suggesting that at least one "extra subunit" was not incorporated into the channel complex. In addition, the solubilized recombinant channel complex formed by tandems was larger in size and more heterogeneous than that formed by the native MscL channel.

The properties of CNG channels are finely adjusted to the specific functions these channels subserve in photoreceptors and olfactory neurons. The number and types of subunits in a channel complex determine the electrophysiological properties of CNG channels. The A and B subunits harbor different functional domains important for the activation by ligands, ion permeation, modulation by Ca^{2+}/Calmodulin (CaM), tethering to other proteins (for review Kaupp and Seifert, 2002), and cellular trafficking (Mallouk et al., 2002; Trudeau and Zagotta, 2002a). For example, the GARP part of the B1 subunit (Colville and Molday, 1996; Körschen et al., 1995, 1999) tethers the CNG channel to the rim of discs by interaction with peripherin (Poetsch et al., 2001). Our results imply that this contact is established by a single B1 subunit. The B1 subunit (Hsu and Molday, 1993, 1994) also carries two CaM binding sites; the site in the

N-terminal region mediates modulation of cGMP sensitivity by Ca^{2+}/CaM (Grunwald et al., 1998; Weitz et al., 1998). This CaM site interacts with a C-terminal region in the A1 subunit; binding of CaM to the site in B1 disrupts the interaction (Trudeau and Zagotta, 2002b). A 3A1-1B1 stoichiometry implies that the three A1 sites might interact with one CaM binding site in B1. Alternatively, one A1 site might interact with B1 and two A1 sites are not engaged. A corollary of this mechanism is that A1 subunits are nonequivalent.

The gating properties of CNG channels suggest that the subunits are arranged as two functional dimers (Liu et al., 1998). A low-resolution structure of the rod CNG channel is lending structural weight to the idea that subunits function together as pairs (Higgins et al., 2002). Given a 3A1-1B1 stoichiometry, the two dimers are structurally and perhaps also functionally nonequivalent.

The olfactory CNG channel is composed of three different subunits: A2, A4, and B1b, a short splice variant of the rod B1 that is lacking the GARP part (Dhallan et al., 1990; Ludwig et al., 1990; Bradley et al., 1994; Liman and Buck, 1994; Sautter et al., 1998; Bönigk et al., 1999). The heterologous expression of various combinations of subunits gives rise to distinct channels. However, only the coexpression of all three subunits produces CNG channels with properties similar to those of the native olfactory CNG channel (Bönigk et al., 1999). In particular, the speed and sensitivity of Ca^{2+}/CaM modulation is only recapitulated when all three subunits are present (Bradley et al., 2001; Munger et al., 2001). The A2 subunit carries one high-affinity CaM binding site (Liu et al., 1994), and the B1b subunit carries two different CaM binding sites (Weitz et al., 1998; Grunwald et al., 1998). Thus, in contrast to the rod CNG channel, modulation of the olfactory CNG channel might involve a complex interplay between several CaM molecules and different CaM binding sites on different subunits. The crosslinking technique might be also suitable to unravel the subunit stoichiometry in olfactory CNG channels and thereby constrain the number of possible interactions between functional domains.

Experimental Procedures

Purification of CNG Channel from Rod Outer Segments (ROS)

ROS were prepared from dark-adapted bovine retina as described (Schnetkamp and Daemen, 1982) and stored in 10 mM HEPES-NaOH (pH 7.4), 1 mM DTT, 1 mM PMSF, and 1 mM Pefabloc. ROS membranes were stripped of soluble proteins by hypotonic lysis and washing under dim red light. Membranes (~10 mg/ml rhodopsin) were diluted 10-fold in a hypotonic buffer containing 10 mM HEPES-NaOH (pH 7.4), 2 mM DTT, and 2 mM EDTA. The suspension was centrifuged for 20 min at 100,000 × g and the pellet was resuspended in hyptotonic buffer. This procedure was repeated three times. The final pellet was solubilized in a buffer containing 18 mM CHAPS, 10 mM HEPES-NaOH (pH 7.4), 200 mM NaCl, 2 mM DTT, 2 mM $CaCl_2$, 25% (v/v) glycerol, and 2 mg/ml soybean phosphatidylcholine. Nonsolubilized material was removed by centrifugation (100,000 × g, 60 min, 4°C). The CNG channel was purified by CaM-affinity chromatography (Hsu and Molday, 1993). CaM-agarose was equilibrated with running buffer containing 15 mM CHAPS, 10 mM HEPES-NaOH (pH 7.4), 150 mM NaCl, 2 mM DTT, 0.5 mM $CaCl_2$, 25% (v/v) glycerol, and 10 μg/ml soybean phosphatidylcholine. After loading of solubilized protein, the column was washed with 10 volumes of running buffer. The channel protein was eluted by replacing the calcium in the running buffer by 0.5 mM EDTA. Fractions were collected and analyzed by Coomassie staining of SDS polyacrylamide gel and Western blot analysis using antibodies against the A1 and B1 subunits. For the thiol-specific crosslinking, purification of the CNG channel was carried out with no DTT present during the elution of the channel protein from the column.

Amino-Specific Crosslinking of Purified CNG Channel

The purified CNG channel was incubated with 0.5 mM of the amino-specific crosslinker Bis(sulfosuccinimidyl)suberate (BS^3) at room temperature. The crosslink reaction was terminated after different incubation times by adding SDS sample buffer (62.5 mM Tris-Cl [pH 6.8], 2% SDS, 10% (v/v) glycerol, 1% (v/v) β-mercaptoethanol, 0.01% Bromphenol Blue).

Thiol-Specific Crosslinking of Purified CNG Channel

The purified CNG channel was incubated with 5 μM of the thiol-specific crosslinker 1,4-Bismaleimidyl-2,3-dihydroxybutane (BMDB) at room temperature. The crosslink reaction was terminated after different incubation times by adding SDS sample buffer. Crosslink products were analyzed by SDS-PAGE and Western blot analysis.

Thiol-Specific Crosslinking of the CNG Channel in ROS Membranes

Membranes were obtained by hypotonic lysis of ROS in 10 mM HEPES-NaOH (pH 7.4), 1 mM EDTA, 1 mM DTT, and the protease inhibitors aprotinin (5 μg/ml), leupeptin (5 μg/ml), and E64 (2.2 μg/ml), followed by centrifugation at 100,000 × g for 25 min at 4°C. The membranes were washed twice in the same buffer and another two times in the absence of DTT. Crosslinking of ROS membranes was carried out in dim red light.

Hypotonically washed membranes were incubated with the thiol-modifying reagent N-ethylmaleimide (NEM) to block all accessible thiol groups of the CNG channel and other membrane proteins. Incubation was terminated by addition of 5 mM DTT. Excess DTT was removed by washing the membranes four times with isotonic buffer (10 mM HEPES-NaOH [pH 7.4], 100 mM NaCl, 1 mM EDTA, and protease inhibitors, see above). The CNG channel was activated by adding 50 μM 8-Br-cGMP to the suspension (0.2 mg/ml rhodopsin). The crosslinking reaction was started by incubation with BMDB (50 μM) at room temperature. Intermediate crosslink products were identified by termination of the reaction with 500 μM DTT in aliquots of the sample at various times. Crosslink products were analyzed by SDS-PAGE and Western blotting.

Amino-Specific Crosslinking of the CNG Channel in ROS Membranes

Hypotonically washed membranes were incubated with 0.5 mM of the amino-specific crosslinking reagent BS^3 at room temperature (5 mg/ml rhodopsin). Intermediate crosslink products were identified by termination of the reaction in aliquots of the sample at various times with 500 mM Tris-HCl (pH 7.5). Crosslink products were analyzed by SDS-PAGE and Western blotting.

Western Analysis of Crosslink Products

Crosslink products were analyzed by SDS-PAGE and Western blot analysis. In order to determine the apparent M_w we used the "High Molecular Weight Calibration Kit" from Pharmacia (53–212 kDa). For a protein standard with a M_w higher than 212 kDa, we crosslinked myosin heavy chains (Hu et al., 1989). The M_w of the myosin dimer and trimer are 424 kDa and 636 kDa, respectively. In earlier experiments, not shown here, nebulin (760 kDa) from rabbit muscle was used as an additional marker protein. The results obtained with oligomeric myosin or nebulin as markers were similar. Marker proteins on Western blots were stained with Amido Black dye. Western blots were developed with the ECL system (Amersham). The M_w of each crosslink product was determined by linear interpolation plotting the log M_w of the standard proteins against their relative mobility R_f on SDS polyacrylamide gels. The reproducibility of calibration curves is illustrated in the figure below.

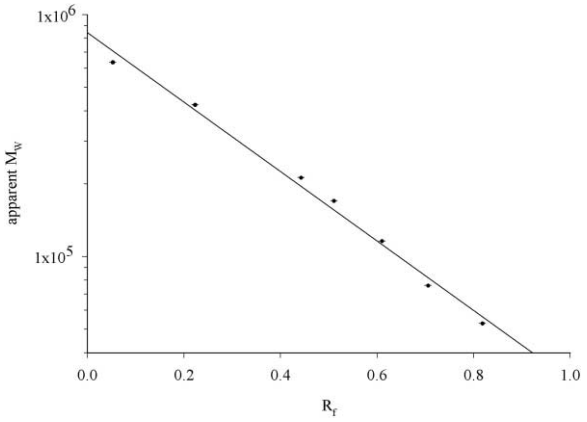

Figure 7. Standard Calibration Curve of Marker Proteins Used in SDS-PAGE

Apparent M_W (ordinate) versus mean values of the relative mobility R_f (abscissa) of seven marker proteins (high molecular weight standard and the myosin dimer and trimer). Standard deviations are indicated as bars (n = 10).

Monoclonal and Polyclonal Antibodies against the CNG Channel

Anti-A1 Antibodies

Polyclonal antibody FPcK39 was obtained from a rabbit immunized with a fusion protein between the maltose binding protein (MBP) and the cGMP binding site of the A1 subunit (amino acids 482–615). The rat monoclonal antibody UED7D3 was produced by immunization with a peptide (amino acids 644–690, coupled to keyhole limpet hemocyanin) and fusion of immune spleen cells according to standard procedures.

Anti-B1 Antibodies

Polyclonal antibody FPcK21 was obtained from a rabbit immunized with a fusion protein between MBP and the entire N-terminal domain of the B1′-part (amino acids 574–763). The antibody was purified by affinity chromatography using the fusion protein coupled to CNBR-Activated Sepharose (Pharmacia). Antibodies against MBP were removed by a second affinity chromatography with MBP coupled to CNBR-Activated Sepharose. Polyclonal antibody FPcK52 was obtained from a rabbit immunized with recombinant GARP2 (amino acids 1–291). The antibody was partially purified by affinity chromatography using Protein A-Sepharose (Pharmacia). The different epitopes of the antibodies are marked in Figure 1A.

Acknowledgments

We thank A. Neef and R. Seifert for critical reading of the manuscript and helpful discussions. We thank R.S. Molday (Vancouver) for the anti-Na^+/Ca^{2+}-K^+ exchanger antibody (PMe 2D9) and G.H. Travis (Los Angeles) for providing the anti-RDS antibody (peripherin). Supported by the Strategy Fund of the Helmholtz Association of Research Centers and the German Research Foundation.

Received: October 11, 2002
Revised: November 13, 2002
Published online: November 20, 2002

References

Bönigk, W., Altenhofen, W., Müller, F., Dose, A., Illing, M., Molday, R.S., and Kaupp, U.B. (1993). Rod and cone photoreceptor cells express distinct genes for cGMP-gated channels. Neuron *10*, 865–877.

Bönigk, W., Bradley, J., Müller, F., Sesti, F., Boekhoff, I., Ronnett, G.V., Kaupp, U.B., and Frings, S. (1999). The native rat olfactory cyclic nucleotide-gated channel is composed of three distinct subunits. J. Neurosci. *19*, 5332–5347.

Bradley, J., Li, J., Davidson, N., Lester, H.A., and Zinn, K. (1994). Heteromeric olfactory cyclic nucleotide-gated channels: a new subunit that confers increased sensitivity to cAMP. Proc. Natl. Acad. Sci. USA *91*, 8890–8894.

Bradley, J., Reuter, D., and Frings, S. (2001). Facilitation of calmodulin-mediated odor adaptation by cAMP-gated channel subuntis. Science *294*, 2176–2178.

Brown, R.L., Snow, S.D., and Haley, T.L. (1998). Movement of gating machinery during the activation of rod cyclic nucleotide-gated channels. Biophys. J. *75*, 825–833.

Burns, M.E., and Baylor, D.A. (2001). Activation, deactivation, and adaptation in vertebrate photoreceptor cells. Annu. Rev. Neurosci. *24*, 779–805.

Chang, G., Spencer, R.H., Lee, A.T., Barclay, M.T., and Rees, D.C. (1998). Structure of the MscL homolog from *Mycobacterium tuberculosis*: a gated mechanosensitive ion channel. Science *282*, 2220–2226.

Chen, T.-Y., Peng, Y.-W., Dhallan, R.S., Ahamed, B., Reed, R.R., and Yau, K.-W. (1993). A new subunit of the cyclic nucleotide-gated cation channel in retinal rods. Nature *362*, 764–767.

Colville, C.A., and Molday, R.S. (1996). Primary structure and expression of the human β-subunit and related proteins of the rod photoreceptor cGMP-gated channel. J. Biol. Chem. *271*, 32968–32974.

Dhallan, R.S., Yau, K.-W., Schrader, K.A., and Reed, R.R. (1990). Primary structure and functional expression of a cyclic nucleotide-activated channel from olfactory neurons. Nature *347*, 184–187.

Flynn, G.E., and Zagotta, W.N. (2001). Conformational changes in S6 coupled to the opening of cyclic nucleotide-gated channels. Neuron *30*, 689–698.

Gerstner, A., Zong, X., Hofmann, F., and Biel, M. (2000). Molecular cloning and functional characterization of a new modulatory cyclic nucleotide-gated channel subunit from mouse retina. J. Neurosci. *20*, 1324–1332.

Gordon, S.E., and Zagotta, W.N. (1995). Subunit interactions in coordination of Ni^{2+} in cyclic nucleotide-gated channels. Proc. Natl. Acad. Sci. USA *92*, 10222–10226.

Gordon, S.E., Varnum, M.D., and Zagotta, W.N. (1997). Direct interaction between amino- and carboxyl-terminal domains of cyclic nucleotide-gated channels. Neuron *19*, 431–441.

Goulding, E.H., Tibbs, G.R., Liu, D., and Siegelbaum, S.A. (1993). Role of H5 domain in determining pore diameter and ion permeation through cyclic nucleotide-gated channels. Nature *364*, 61–64.

Grunwald, M.E., Yu, W.-P., Yu, H.-H., and Yau, K.-W. (1998). Identification of a domain on the β-subunit of the rod cGMP-gated cation channel that mediates inhibition by calcium-calmodulin. J. Biol. Chem. *273*, 9148–9157.

He, Y., Ruiz, M.L., and Karpen, J.W. (2000). Constraining the subunit order of rod cyclic nucleotide-gated channels reveals a diagonal arrangement of like subunits. Proc. Natl. Acad. Sci. USA *97*, 895–900.

Henn, D.K., Baumann, A., and Kaupp, U.B. (1995). Probing the transmembrane topology of cyclic nucleotide-gated ion channels with a gene fusion approach. Proc. Natl. Acad. Sci. USA *92*, 7425–7429.

Higgins, M.K., Weitz, D., Warne, T., Schertler, G.F.X., and Kaupp, U.B. (2002). Molecular architecture of a retinal cGMP-gated channel: the arrangement of the cytoplasmic domains. EMBO J. *21*, 2087–2094.

Hsu, Y.-T., and Molday, R.S. (1993). Modulation of the cGMP-gated channel of rod photoreceptor cells by calmodulin. Nature *361*, 76–79.

Hsu, Y.-T., and Molday, R.S. (1994). Interaction of calmodulin with the cyclic GMP-gated channel of rod photoreceptor cells. J. Biol. Chem. *269*, 29765–29770.

Hu, D.H., Kimura, S., and Maruyama, K. (1989). Myosin oligomers as the molecular mass standard in the estimation of molecular mass of nebulin (~800 kDa) by sodium dodecyl sulfate-polyacrylamide gel electrophoresis. Biomed. Res. *10*, 165–168.

Kaupp, U.B., and Seifert, R. (2002). Cyclic nucleotide-gated ion channels. Physiol. Rev. *82*, 769–824.

Kaupp, U.B., Niidome, T., Tanabe, T., Terada, S., Bönigk, W., Stühmer, W., Cook, N.J., Kangawa, K., Matsuo, H., Hirose, T., et al. (1989). Primary structure and functional expression from comple-

mentary DNA of the rod photoreceptor cyclic GMP-gated channel. Nature *342*, 762–766.

Körschen, H.G., Illing, M., Seifert, R., Sesti, F., Williams, A., Gotzes, S., Colville, C., Müller, F., Dosé, A., Godde, M., et al. (1995). A 240 kDa protein represents the complete β subunit of the cyclic nucleotide-gated channel from rod photoreceptor. Neuron *15*, 627–636.

Körschen, H.G., Beyermann, M., Müller, F., Heck, M., Vantler, M., Koch, K.-W., Kellner, R., Wolfrum, U., Bode, C., Hofmann, K.P., and Kaupp, U.B. (1999). Interaction of glutamic-acid-rich proteins with the cGMP signalling pathway in rod photoreceptors. Nature *400*, 761–766.

Liman, E.R., and Buck, L.B. (1994). A second subunit of the olfactory cyclic nucleotide-gated channel confers high sensitivity to cAMP. Neuron *13*, 611–621.

Liu, M., Chen, T.-Y., Ahamed, B., Li, J., and Yau, K.-W. (1994). Calcium-calmodulin modulation of the olfactory cyclic nucleotide-gated cation channel. Science *266*, 1348–1354.

Liu, D.T., Tibbs, G.R., and Siegelbaum, S.A. (1996). Subunit stoichiometry of cyclic nucleotide-gated channels and effects of subunit order on channel function. Neuron *16*, 983–990.

Liu, D.T., Tibbs, G.R., Paoletti, P., and Siegelbaum, S.A. (1998). Constraining ligand-binding site stoichiometry suggests that a cyclic nucleotide-gated channel is composed of two functional dimers. Neuron *21*, 235–248.

Ludwig, J., Margalit, T., Eismann, E., Lancet, D., and Kaupp, U.B. (1990). Primary structure of cAMP-gated channel from bovine olfactory epithelium. FEBS Lett. *270*, 24–29.

MacKinnon, R. (1991). Determination of the subunit stoichiometry of a voltage-activated potassium channel. Nature *350*, 232–235.

Mallouk, N., Ildefonse, M., Pagès, F., Ragno, M., and Bennett, N. (2002). Basis for intracellular retention of a human mutant of the retinal rod channel alpha subunit. J. Membr. Biol. *185*, 129–136.

McCormack, K., Lin, L., Iverson, L.E., Tanouye, M.A., and Sigworth, F.J. (1992). Tandem linkage of *Shaker* K^+ channel subunits does not ensure the stoichiometry of expressed channels. Biophys. J. *63*, 1406–1411.

Molday, R.S., and Molday, L.L. (1998). Molecular properties of the cGMP-gated channel of rod photoreceptors. Vision Res. *38*, 1315–1323.

Molokanova, E., Trivedi, B., Savchenko, A., and Kramer, R.H. (1997). Modulation of rod photoreceptor cyclic nucleotide-gated channels by tyrosine phosphorylation. J. Neurosci. *17*, 9068–9076.

Munger, S.D., Lane, A.P., Zhong, H., Leinders-Zufall, T., Yau, K.-W., Zufall, F., and Reed, R.R. (2001). Central role of the CNGA4 channel subunit in Ca^{2+}-calmodulin-dependent odor adaptation. Science *294*, 2172–2175.

Poetsch, A., Molday, L.L., and Molday, R.S. (2001). The cGMP-gated channel and related glutamic acid-rich proteins interact with peripherin-2 at the rim region of rod photoreceptor disc membranes. J. Biol. Chem. *276*, 48009–48016.

Raab-Graham, K.F., and Vandenberg, C.A. (1998). Tetrameric subunit structure of the native brain inwardly rectifying potassium channel K_{ir} 2.2. J. Biol. Chem. *273*, 19699–19707.

Richards, M.J., and Gordon, S.E. (2000). Cooperativity and cooperation in cyclic nucleotide-gated ion channels. Biochemistry *39*, 14003–14011.

Rosenbaum, T., and Gordon, S.E. (2002). Dissecting intersubunit contacts in cyclic nucleotide-gated ion channels. Neuron *33*, 703–713.

Sautter, A., Zong, X., Hofmann, F., and Biel, M. (1998). An isoform of the rod photoreceptor cyclic nucleotide-gated channel β subunit expressed in olfactory neurons. Proc. Natl. Acad. Sci. USA *95*, 4696–4701.

Schnetkamp, P.P.M., and Daemen, F.J.M. (1982). Isolation and characterization of osmotically sealed bovine rod outer segments. Methods Enzymol. *81*, 110–116.

Schulteis, C.T., Nagaya, N., and Papazian, D.M. (1996). Intersubunit interaction between amino- and carboxyl-terminal cysteine residues in tetrameric Shaker K^+ channels. Biochemistry *35*, 12133–12140.

Schwarzer, A., Schauf, H., and Bauer, P.J. (2000). Binding of the cGMP-gated channel to the Na/Ca-K exchanger in rod photoreceptors. J. Biol. Chem. *275*, 13448–13454.

Seifert, R., Eismann, E., Ludwig, J., Baumann, A., and Kaupp, U.B. (1999). Molecular determinants of a Ca^{2+}-binding site in the pore of cyclic nucleotide-gated channels: S5/S6 segments control affinity of intrapore glutamates. EMBO J. *18*, 119–130.

Serre, V., Ildefonse, M., and Bennett, N. (1995). Effects of cysteine modification on the activity of the cGMP-gated channel from retinal rods. J. Membr. Biol. *146*, 145–162.

Shammat, I.M., and Gordon, S.E. (1999). Stoichiometry and arrangement of subunits in rod cyclic nucleotide-gated channels. Neuron *23*, 809–819.

Sukharev, S.I., Schroeder, M.J., and McCaslin, D.R. (1999). Stoichiometry of the large conductance bacterial mechanosensitive channel of *E. coli*. A biochemical study. J. Membr. Biol. *171*, 183–193.

Trudeau, M.C., and Zagotta, W.N. (2002a). An intersubunit interaction regulates trafficking of rod cyclic nucleotide-gated channels and is disrupted in an inherited form of blindness. Neuron *34*, 197–207.

Trudeau, M.C., and Zagotta, W.N. (2002b). Mechanism of calcium/calmodulin inhibition of rod cyclic nucleotide-gated channels. Proc. Natl. Acad. Sci. USA *99*, 8424–8429.

Varnum, M.D., and Zagotta, W.N. (1996). Subunit interactions in the activation of cyclic nucleotide-gated ion channels. Biophys. J. *70*, 2667–2679.

Weitz, D., Zoche, M., Müller, F., Beyermann, M., Körschen, H.G., Kaupp, U.B., and Koch, K.-W. (1998). Calmodulin controls the rod photoreceptor CNG channel through an unconventional binding site in the N-terminus of the β-subunit. EMBO J. *17*, 2273–2284.

Wohlfart, P., Haase, W., Molday, R.S., and Cook, N.J. (1992). Antibodies against synthetic peptides used to determine the topology and site of glycosylation of the cGMP-gated channel from bovine rod photoreceptors. J. Biol. Chem. *267*, 644–648.

Zheng, J., and Zagotta, W.N. (2000). Gating rearrangements in cyclic nucleotide-gated channels revealed by patch-clamp fluorometry. Neuron *28*, 369–374.